Canadian Conference - Pacific Conference on Earthquake Engineering 2023
Vancouver, British Columbia
June 25th – June 30th, 2023

# Evaluating the Impact of Fluid Viscous Dampers on the Seismic Collapse and Loss Assessment of Chilean RC Dual Wall-Frame Buildings

Marco F. Gallegos[1*], Gerardo Araya-Letelier[2], Diego Lopez-Garcia[3] and Carlos Molina Hutt[4]

[1]PhD Candidate, Department of Structural and Geotechnical Engineering, Pontificia Universidad Catolica de Chile, Santiago, Chile, & Visiting International Research Student, Department of Civil Engineering, The University of British Columbia, Vancouver, BC, Canada
[2]Associate Professor, School of Civil Construction, Faculty of Engineering, & Concrete Innovation Hub UC (CIHUC), Pontificia Universidad Catolica de Chile, Santiago, Chile
[3]Associate Professor, Department of Structural and Geotechnical Engineering, & Research Center for Integrated Disaster Risk Management (CIGIDEN) ANID FONDAP 1522A0005, Pontificia Universidad Catolica de Chile, Santiago, Chile
[4]Assistant Professor, Department of Civil Engineering, The University of British Columbia, Vancouver, BC, Canada
[*]mfgallegos@uc.cl (Corresponding Author)

## ABSTRACT

During the 2010 $M_w$ 8.8 earthquake in Chile, with the exception of a few collapse occurrences, reinforced concrete (RC) buildings generally experienced minor structural damage. Nevertheless, the event caused significant economic losses partly due to damage to their nonstructural building components and contents. This observation suggests a need for higher levels of resilience in buildings, which might be achieved by incorporating seismic protection systems, such as fluid viscous dampers (FVDs), into the structural system. This study assesses the effect of FVDs on the seismic performance of code-conforming high-rise RC dual wall-frame office buildings. As a case study, a 16-story archetype building representative of the Chilean state of design and construction practice was selected. Two cases were analyzed: i) the archetype without dampers (i.e., conventional design), and ii) the same archetype equipped with supplemental FVDs. The archetypes were examined considering the latest developments in performance-based earthquake engineering. Three-dimensional nonlinear models, developed in Perform-3D, were subjected to incremental dynamic analyses using a set of hazard-consistent Chilean subduction ground motions to evaluate the collapse fragility of the case study buildings. Additionally, a loss assessment was carried out using the FEMA P-58 methodology at four distinct hazard levels with return periods of 72, 475, 2475, and 4975 years. The convenience of the performance improvement strategy was quantitively evaluated in terms of reduction in collapse risk and expected direct economic losses. The results revealed that the archetype equipped with FVDs exhibits a higher level of collapse capacity and smaller levels of economic losses despite higher initial construction costs. The 50-year probability of collapse was almost halved when the dampers were incorporated. Similarly, reductions in earthquake-induced repair costs were on the order of ~50% with respect to those from a conventional design. Greater cost decreases were observed under extreme shaking intensities (e.g., 2475 and 4975-year return periods) than under more frequent earthquakes (i.e., 72 and 475-year return periods).

Keywords: RC dual wall-frame office building, fluid viscous damper, collapse assessment, loss assessment, Chilean subduction earthquakes.

## INTRODUCTION

While modern seismic building codes aim to avoid collapse under extreme earthquakes, extensive structural and non-structural damage may occur. Recent major seismic events in Chile and New Zealand have shown that the 'life safety' performance level in modern codes has been successfully achieved with relatively few collapsed buildings. However, the earthquake-induced economic losses due to the widespread damage, demolitions, and downtime in engineered buildings were significant. For example, for the $M_w$ 8.8, 2010 Chile earthquake, estimates of economic losses were around US $30 billion (18% of the 2010 Chilean gross domestic product, GDP), and the international airports in Santiago and Concepcion were out of service for weeks due to nonstructural damage [1]. While, for the $M_w$ 6.3, 2011 New Zealand earthquake, the total losses were estimated to be over US $15 billion (10% of the 2011 New Zealand GDP), and about 50% of all the concrete and masonry buildings in

Christchurch's Central Business District were unusable because they exhibited significant damage, where the District area was closed for several months [2].

These significant consequences suggest that to meet the expectations of modern society, the built environment needs to achieve enhanced seismic performance beyond the minimum current code requirements. Traditionally, such levels of higher building performance are reached by improving the lateral load-resisting system, e.g., stiffening and strengthening the structural elements or incorporating seismic protection systems, to reduce the damage to both structural and nonstructural components. In either case, enhancing the structural system typically results in greater construction costs, requiring cost-benefit analyses to understand the trade-off between higher initial investments and a future reduction in earthquake-induced economic losses.

Most mid- and high-rise buildings in Chile have reinforced concrete (RC) structural systems. Based on the building permit statistics provided by the Chilean National Institute of Statistics [3], nearly 8000 RC buildings of three stories and higher were constructed between 2002 and 2020. From this inventory, 90% have shear-wall systems, whereas 10% have dual wall-frame systems, i.e., core structural walls and perimeter moment frames. Although little used in Chile, the advantage of having floor plans with larger open spaces with adequate structural performance makes dual system structures commonly used in other prone-earthquake regions for tall buildings or those constructed on poor soils.

After the 2010 earthquake, seismic protection systems have gained popularity within the Chilean engineering community as a new technological solution for damage control, content protection, and occupant comfort in RC buildings [4]. Energy-dissipation devices, such as fluid viscous dampers (FVDs), are commonly used to seismically enhance buildings. Adoption of FVDs in reinforced concrete dual wall-frame (RCWF) buildings is common as it enables relative architectural freedom in the floor plan, as dampers can be installed within the spans between columns in the perimeter moment frames. FVDs allow energy dissipation, substantially reducing the proportion of seismic energy that must be dissipated by the structure, improving the seismic response, but also increasing initial construction costs. Consequently, some concerns remain regarding the cost-benefit of Chilean RCWF buildings equipped with FVDs.

The performance-based earthquake engineering (PBEE) framework enables evaluating the probable seismic performance of structures over their operational life. The methodology proposed by the Pacific Earthquake Engineering Research (PEER) Center allows the assessment of new or existing buildings with a realistic and reliable understanding of the risks to life, occupancy, and economic loss that might occur in future earthquakes. In their FEMA P-58 [5] implementation, seismic performance is expressed in terms of decision variables (i.e., performance metrics) that can be understood by decision-makers, such as collapse probability, direct economic losses (i.e., building repair or replacement costs), repair time, and environmental impacts. Despite the availability of these tools, little information is available on the expected collapse risk and earthquake-induced losses of RC buildings equipped with FVDs, especially in regions prone to subduction earthquakes, such as Chile.

To address these concerns in the Chilean engineering community as well as in other countries located along the Pacific Ring of Fire, this study evaluates the effect of FVDs on the seismic collapse capacity and expected economic losses of code-conforming RCWF buildings. As a case study, a high-rise 16-story archetype office building representative of Chile's current design and construction practice was equipped with supplemental FVDs. The archetypes were analyzed considering the latest developments in the PBEE framework. Three-dimensional nonlinear models, implemented into Perform-3D software, are subjected to incremental dynamic analyses (IDAs) for a set of hazard-consistent Chilean subduction ground motions (GMs) to evaluate the building's collapse fragility. Additionally, following the FEMA P-58 methodology, intensity-based assessments at four hazard intensity levels, i.e., return periods of 72, 475, 2475, and 4975 years, were conducted. Besides the use of FVDs, the use of enhanced nonstructural components was also explored. Finally, the benefits of the proposed performance improvement strategy are quantitatively assessed in terms of decreases in collapse risk and earthquake-induced direct economic losses while considering the higher initial construction costs associated with the use of FVDs.

## ARCHETYPE BUILDINGS

### The Chilean Practice and Prescriptive Design Procedures

Chilean RCWF buildings are mostly used for office occupancy. The floor system typically consists of flat post-tensioned slabs with 17 to 20 cm thickness and 8 to 10 m spans. Thus, perimeter moment frames are usually intermediate moment frames (IMFs) designed to take no more than 25% of the prescribed seismic load, whereas core walls are special structural walls. At the conceptual stage, the walls' cross sections (specifically the thicknesses) are defined based on the 'wall density' criterion commonly used in engineering practice. Wall density, defined as the ratio of the wall area in each principal direction at the base floor level to the total area of all floors above that level, must be larger than 0.1% [6]. This criterion is intended to provide enough strength and stiffness to the structure and to limit the average shear stress and average compression in shear walls.

Pre-2010 RC buildings were designed following the Chilean codes NCh 430 'Design of Reinforced Concrete Structures' [7], and NCh 433 'Seismic Design of Buildings' [8]. After the 2010 earthquake, some deficiencies in the Chilean provisions were detected, such as the lack of requirements restricting irregularities in building height, the use of slender shear walls with thickness less than 150 mm, and the non-obligation to adequately confine shear wall boundary elements [9]. In 2011, two regulatory documents upgraded the previous prescriptive codes. The document DS 60 [10] updated the concrete design requirements adopting the code ACI 318S-08 with some local modifications for shear wall design, whereas the document DS 61 [11] introduced the average seismic shear-wave velocity from the surface to a depth of 30 meters ($Vs_{30}$) as a soil classification parameter, and modified the earthquake demands imposed over building structures. The latter document adopts two different levels of earthquake magnitudes for the design of walls. One for strength design, similar to the former code acceleration spectra [8] originally calibrated to the 1985 earthquake ($M_w$ 8.0), and a new higher-level earthquake for structural damage control, calibrated for the roof displacement demands observed in the 2010 earthquake ($M_w$ 8.8). Further details about the Chilean practice of seismic design for RC buildings can be found in Lagos et al. [6].

In recent years, new codes have been developed to deal with the seismic design of buildings equipped with seismic protection systems such as the Chilean codes NCh 2745 [12] for buildings with seismic isolation, and NCh 3411 [13] for buildings with passive energy dissipated devices. Both documents are based on the requirements of the US code ASCE 7-10. The NCh 3411, recently introduced in 2017, has scarcely been implemented in real RC buildings.

**Archetype Selection and Structural Design**

The characteristics of the archetype building used in this study were defined on the basis of statistical data from the RC building inventory compiled by the Chilean National Institute of Statistics [3], coupled with knowledge of the state of design and construction practice in the region. This study focused on the segment of high-rise buildings (i.e., from 10 to 24 stories) for two reasons. First, the number of these buildings has grown considerably in recent years, and there is little information about their anticipated seismic performance. Second, high-rise buildings might have a significant contribution of higher modes to the seismic response. This fact generates a more variable distribution of story drift ratios, which might affect collapse performance and economic losses [14].

A 16-story office building (occupation category II [8]) located in Santiago (moderate seismicity zone [8]) over stiff soil (500 m/s $\leq Vs_{30} <$ 900 m/s [11]) is considered (Figure 1a). The building plan dimensions are 24 m × 40 m (960 m$^2$), with a typical span length of 8.0 m. The archetype has three underground levels surrounded by perimeter basement walls. Post-tensioned slabs are considered on all floor levels. The structural system consists of two core C-shaped shear walls, and IMFs located at the perimeter (Figure 1b). This archetype is labeled as the benchmark archetype building, BAB, hereinafter.

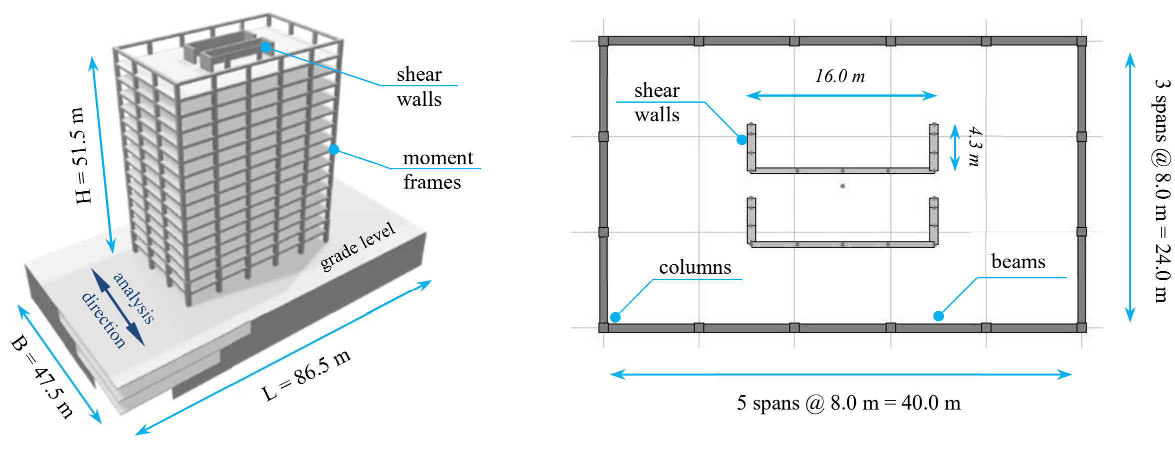


*Figure 1. 16-story benchmark archetype building (BAB): (a) 3D view, (b) plan layout.*

The BAB was designed utilizing the modal response spectrum method where the seismic forces are defined by an elastic spectrum divided by a period-dependent response modification factor ($R_{eff}$) [8], [11]. The natural period in the transverse direction is 1.93 s ($R_{eff}$ = 3.7), whereas 0.83 s ($R_{eff}$ = 4.7) for the longitudinal direction. Design of concrete members followed the post-2010 code [10]. As required by the code, boundary elements (special, SBE, and ordinary, OBE) were provided at the ends of the flanges of the shear walls. SBEs were provided only at the first two stories below grade level and at the first three stories above grade level. Further details of the archetype geometry, member cross-sections, and design particularities of the BAB can be found in Gallegos et al. [15].

Regarding the design of the archetype building equipped with FVDs (BAB+FVD), the code NCh 3411 [13] was followed. Although the provisions allow a decrease of the seismic base shear demand due to the increase of damping provided by supplemental FVD (by means of reduction factors), the common engineering practice prefers not to reduce the demand. Based on the expert opinion of Chilean practitioners, it was decided to include additional dampers to the benchmark structure conventionality designed with the NCh 433 [8], [11]. However, further verifications were needed to evaluate the performance of the complete system (i.e., structural system + damping system) for different levels of seismic demand. The NCh 3411 requires that the dynamic response of the structure and elements of the damping system shall be confirmed by using the nonlinear response-history (NLRH) procedure with a set of compatible ground motions for two demand levels. First, a design earthquake (denoted as SDI in [13]), with a probability of exceedance of 10% in 50 years, was used to evaluate the flexural-axial stress demands in columns indicating that the columns adjacent to the FVD did not need to be reinforced. Second, a maximum possible earthquake (denoted as SMP in [13]), with a probability of exceedance of 10% in 100 years, was used to evaluate the devices verifying that the maximum force and stroke were not exceed.

Chilean RC buildings are characterized by a stiff structural system; therefore, a motion amplification configuration was required to amplify the small relative motion at the two ends of the dampers. In this sense, FVDs were placed every three stories starting from the grade level in the transverse direction of the building (i.e., critical direction). FVDs were arranged in a horizontal configuration attached with inverted Chevron steel braces. A total number of 20 FVDs were required (two pairs every three stories, five pairs per perimeter side). Based on the recommendation of practitioners, a nonlinear damper with properties of a maximum output force ($F_d$) of 50 ton, and velocity exponent ($\alpha$) of 0.35 was selected (a single damper type was used). Specifications for $\alpha$ typically range from 0.3 to 0.5 for seismic energy dissipation [16]. The criterion of $F_d \leq 50$ ton is based on limiting the forces transferred from the FVDs to the post-tensioned slabs to avoid strengthening of elements that might result in additional construction costs. The damping constant ($c_d$) was calculated considering the average of the peak story relative velocities (i.e., maximum relative response at every three stories for each NLRH analysis) for the SDI demand level. The FVD's behavior is idealized as a pure dashpot as shown in the constitutive Eq. (1), providing the relationship between the damper output force and relative velocity ($\dot{x}$). Since the FVDs do not add stiffness to the structure, natural periods remain constant.

$$F_d(\dot{x}) = sign(\dot{x})\ c_d\ |\dot{x}|^{\alpha} \tag{1}$$

**Nonlinear Modeling**

NLRH analyses requires that the members of the structural system and the dampers be modeled as nonlinear elements. The two tridimensional mathematical models were implemented using Perform-3D [17] following latest guidelines [18], [19]. Figure 2 depicts the Perform-3D models. This software was selected since it provided a good balance between accuracy and computational cost. Recent research has utilized this software to model Chilean RC shear wall buildings [20], [21] indicating that it is adequate for the seismic analysis of the type of archetypes considered in this study.

The slender shear walls were simulated with the 'shear wall' element. The element formulation combines two models to simulate wall behavior: i) a fiber-based section model with nonlinear concrete and steel fibers, and ii) a uniform shear layer, with a one-dimensional nonlinear shear model. Material properties of the wall cross-section fibers were defined using the uniaxial constitutive relationship (i.e., stress vs. strain backbone curve) YULRX (Y: yielding, U: ultimate, L: loss, R: residual, X: maximum), considering unloading and reloading stiffnesses degradation by means of energy dissipation and stiffness reduction factors. The shear layer was defined by a bilinear stress-strain backbone curve. On the other hand, beams and columns were modeled as 'frame type' elements with fiber-based plasticity regions at both ends and a linear-elastic region in between. YULRX backbone curves were also adopted to model the uniaxial stress-strain relationships of concrete and steel materials. Expected material strengths and member stiffnesses were considered. Geometric nonlinearity was contemplated including P-delta effects in walls and columns. Further details of the BAB modeling can be found in Gallegos et al. [15].

The FVDs were simulated with the 'viscous bar' element based on the Maxwell model, which includes a linear elastic bar component and a fluid damper component in series [17]. The bar component reflects the global in-series stiffness of a brace element, its connections, and the internal stiffness of the FVD. The damper component represents the main characteristics of the FVD devices. As shown in Eq. (1), two input values are required to define a FVD ($c_d$ and $\alpha$) that were specified in the design stage. The effectiveness of the numerical model of nonlinear viscous damper under dynamic earthquake loading at a component level was validated with the 'viscousdamper' element implemented in OpenSees [22]. The latter numerical model had been validated with previous experimental studies of a dynamically tested full-scale building at the E-Defense facility [23]. Recent studies have demonstrated the suitability of the Perform-3D 'viscous bar' element for applications in mid- and high-rise buildings equipped with FVDs subjected to seismic loading [24]. Figure 2b shows a 3D view of the archetype building equipped with FVDs (BAB+FVD), where the 20 dampers located in the perimeter transverse frames are shown in red. Figure 2c shows a lateral view with the arrangement of the dampers in a horizontal configuration and the inverted Chevron steel braces.

Basement walls and steel braces were modeled as elastic elements because no nonlinear behavior is expected in those elements. Post-tensioned slabs were not explicitly incorporated into the analytical models; instead, rigid diaphragms were defined at all floor levels, while accounting for the self-weight and mass of the slabs. Most energy dissipation was modeled directly through the hysteretic force-deformation response of the structural components and FVDs. Equivalent viscous modal damping was set equal to 2.4% for all modes, and additional Rayleigh damping was set equal to 0.1% at 0.2 $T_1$ and at 1.5 $T_1$. The columns and walls were assumed to be fixed at the base level.

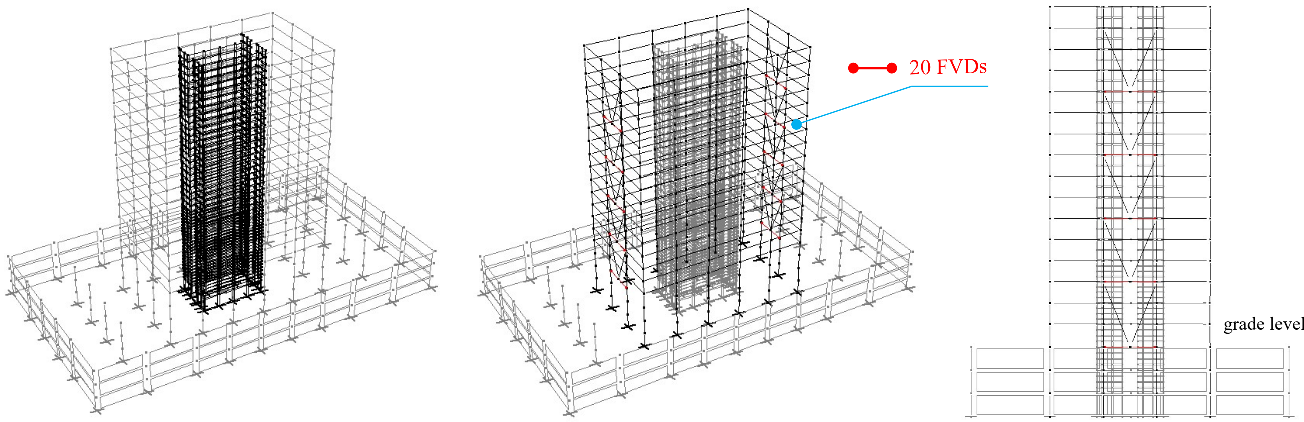


*(a)* *(b)* *(c)*

*Figure 2. Perform-3D models: (a) benchmark archetype building (BAB), (b) archetype building with FVDs (BAB+FVD), (c) lateral view of BAB+FVD in transverse direction.*

## PERFORMANCE ASSESSMENT

The objective of this study is twofold: i) to assess the collapse fragility of the case study building with and without FVDs, and ii) to evaluate building performance using the FEMA P-58 methodology at four distinct hazard levels with probabilities of exceedance equal to 50%, 10%, 2%, and 1% in 50 years, i.e., service level earthquake (SLE), design basic earthquake (DBE), maximum considered earthquake (MCE), and very rare earthquake (VRE), respectively.

### Seismic Hazard and GM Selection

A probabilistic seismic hazard analysis was performed within the computational platform SeismicHazard [25], integrating the seismic source model defined by Poulos et al. [26] as well as the ground motion models proposed by Montalva et al. [27] and by Idini et al. [28]. As a result, site-specific hazard curves for different periods were obtained for the archetypes located in Santiago on stiff soil. A uniform hazard spectrum with a 2% probability of exceedance in 50 years, and then a Conditional Spectrum (CS) was rigorously constructed. The latter was selected as the target spectrum in this study. Utilizing the Chilean strong motion database 'SIBER-RISK' [29], a hazard-consistent set of 44 subduction GMs components was selected and scaled to match the target mean, variance, and correlations of spectral acceleration values, $S_a(T)$. This suite of ground motions, which includes acceleration records from the 1985 seismic event to the latest mega-thrust earthquakes of 2010, 2014 and 2015, was used to conduct IDA to develop the collapse fragility of the archetype buildings. A subset of these results, representative of SLE, DBE, MCE and VRE were then used for the FEMA P-58 assessment.

As will be discussed in more detail in the next section, each GM was applied to transverse direction of the building (i.e., only the response in the weak direction was analyzed). Since the natural periods of vibration for both buildings (i.e., BAB and BAB+FVD) remained the same, the CS and the set of 44 ground motions are identical for both cases.

### Incremental Dynamic Analysis and Comparison of Responses

IDA involved numerous NLRH analyses that were performed using the previously selected set of GMs systematically scaled to increase earthquake intensity until collapse. The adopted intensity measure (IM) is the spectral acceleration at the fundamental period of the structure, $S_a(T_1)$. The structural models were subjected to a set of NLRH analyses with ground motions scaled with increasing $S_a(T_1)$ at steps of 0.05 g until collapse. To reduce the computational burden, the dynamic analyses were performed only along the direction of the shorter horizontal plan dimension, which is the critical direction.

While several parameters need to be considered to completely evaluate structural response, it is common to describe performance by means of engineering demand parameters (EDPs) such as: i) peak story drift ratio, PSDR; ii) peak story tangential drift ratio, PSDRt; iii) peak residual drift ratio, PRDR; and iv) peak floor acceleration, PFA. PSDRt, also called damageable story drift, eliminates rigid body rotation within wall panels, and is considered a better proxy for wall damage than PSDR in mid- to high-rise shear wall buildings [30]. Figure 3 presents the median EDPs for the four shaking intensities SLE, DBE, MCE, and VRE. Solid lines represent the response of BAB, whereas dashed lines represent the response of BAB+FVD. The figure legend indicates the closest $S_a(T_1)$ value (from the IDA) associated to the corresponding intensity level from the fundamental period hazard curve of the archetypes. The $S_a(T_1)$ values are 0.05 g, 0.15 g, 0.35 g, and 0.45 g for the return periods, Tr, of 72, 475, 2475, and 4975 years, respectively.

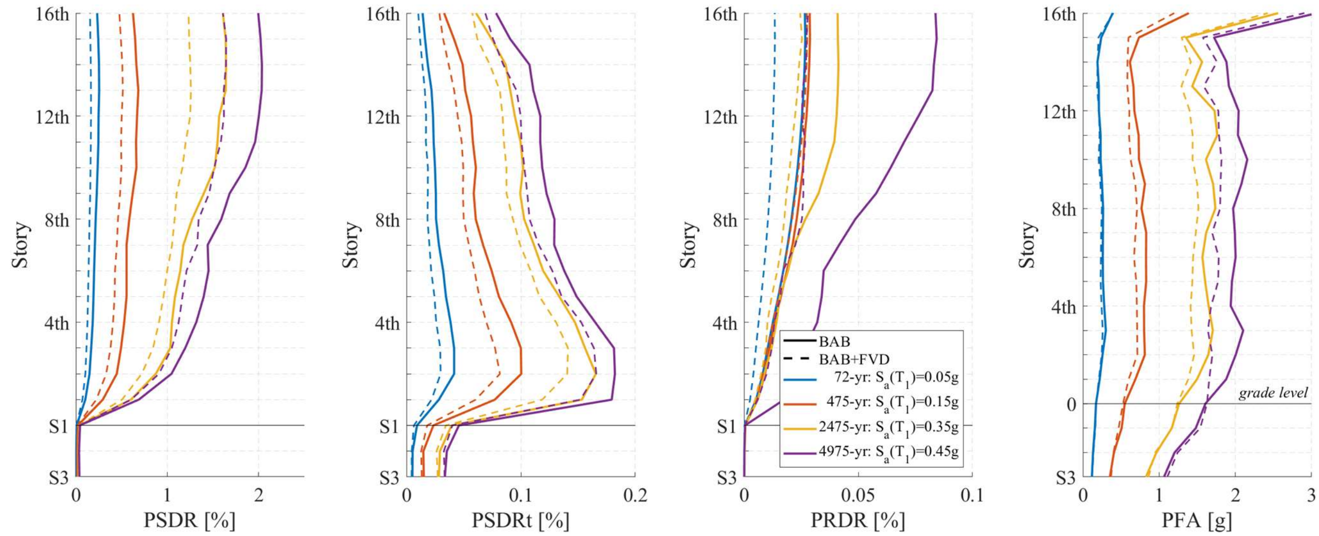


*(a)* *(b)* *(c)* *(d)*

*Figure 3. Structural Response in terms of: (a) peak story drift ratio, (b) peak story tangential drift ratio, (c) peak residual drift ratio, (d) peak floor acceleration.*

In general terms, as the shaking intensity rises, results show increasing reductions in the median responses comparing BAB to BAB+FVD. This fact highlights again the advantage of incorporating energy dissipating devices in the building response decrease. Results also show minimal differences in the response reduction at SLE intensity, especially for floor accelerations (Figure 3d). This behavior was expected since for a low $S_a(T_1)$ value equal to 0.05g both structures remain elastic (for nearly all ground motions) and the FVDs were not yet activated in most of the cases.

From drift plots in Figure 3a and 3b some interesting aspects are observed. First, for both archetypes at SLE and DBE intensities, story drift ratios are below 0.3% and 0.7%, respectively, while tangential story drifts are below 0.05% and 0.1%, respectively. Since RC buildings are expected to present noticeable damage (i.e., large cracks in walls) at drifts slightly larger than 1%, elastic behavior is expected at these levels of excitation. Second, even for extreme events (i.e., MCE and VRE intensities), total and tangential drifts are lower than 2.0% and 0.2%, respectively. These results confirm how stiff Chilean RC buildings are and these results are consistent with the observed lack of structural damage in recent earthquakes for service and design levels.

It is worth noting that most of the medians in residual drift response (Figure 3c) have a maximum value of 0.02%, except for BAB at MCE and VRE intensities. This value could be considered within typical construction tolerances. On the other hand, BAB+FVD at MCE and VRE intensities significantly reduce the mean residual drift. Based on that, FVDs seem to be an effective strategy in limiting residual displacements after extreme events, an important consideration in judging the post-earthquake safety of a building and the economic feasibility of repair or demolition [5].

From the PFA medians in Figure 3d, significant decreases in the BAB+FVD response are noted at MCE and VRE intensities, especially for stories above the ground level until up the 15$^{th}$ floor. Moreover, the impact of supplemental FVDs is evidenced in a more uniform distribution of the peak values over the height of the building for all shaking intensities. This might represent an advantage in the seismic performance of the seismically enhanced building avoiding the concentration of damage at certain floors in contents and acceleration-sensitive nonstructural components, such as ceilings or pipes.

In addition to the reductions in the EDP median values comparing BAB and BAB+FVD, it is noted that the dispersion is also reduced for most of the cases at the four excitation levels. As an example, Figure 4 shows decreases in the dispersion response for PSDR (Figure 4a and 4b) and PFA (Figure 4c and 4d) at the VRE intensity. The shaded limits represent the full range of responses, and 16$^{th}$-84$^{th}$ percentiles. Solid lines for BAB, whereas dashed lines for BAB+FVD.

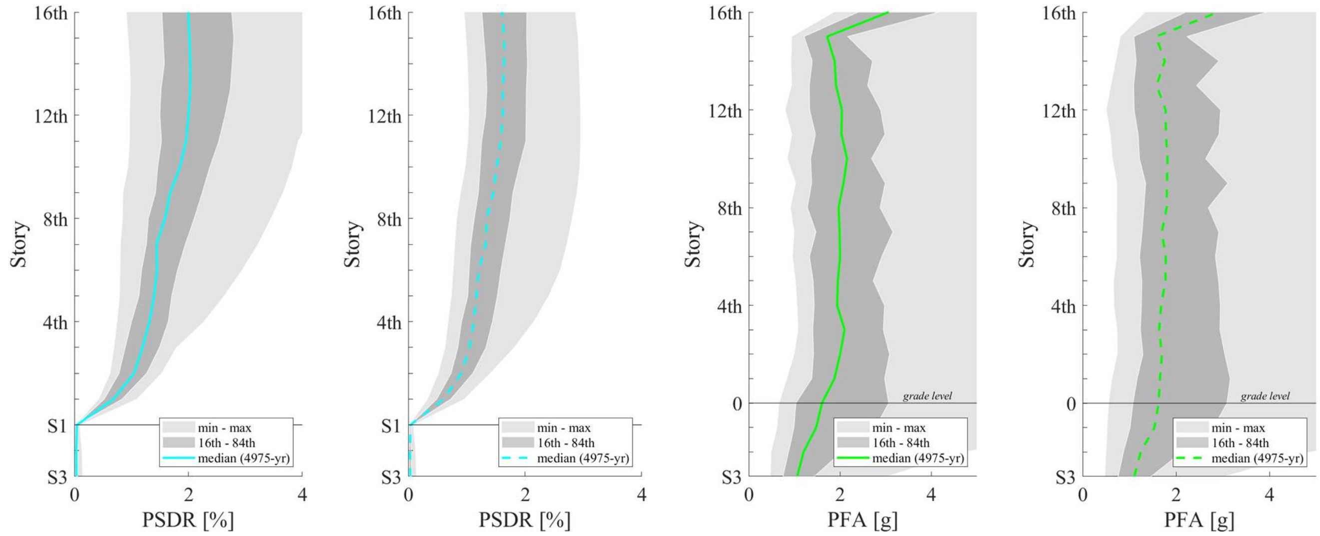


*(a)* *(b)* *(c)* *(d)*

*Figure 4. Structural Response for Tr=4975 years in terms of peak story drift ratio: (a) BAB, (b) BAB+FVD; and peak floor acceleration: (c) BAB, (d) BAB+FVD.*

**Collapse Assessment**

Predicting earthquake-induced collapse requires identification of all possible modes of collapse. This study assessed non-simulated and simulated structural collapse. For details about the collapse criteria used, please refer to Gallegos et al. [15]. Unlike the BAB, for the BAB+FVD, simulated failures on the first-story columns were detected by local response in the longitudinal reinforcement (i.e., buckling) and concrete (i.e., crushing) fibers derived from compression demands. It must be mentioned that other measures of collapse, such as numerical instability or excessive increases in story drift demands for small increases $S_a(T_1)$ were not observed.

One of the principal results of the assessment was the collapse fragility function, which is the probability of triggering collapse conditioned on a specific ground motion intensity measure. For each archetype, the $S_a(T_1)$ values that triggered collapse were recorded for each GM. Assuming a lognormal probability function, the median collapse capacity, $\hat{\theta}$, and the dispersion, $\hat{\beta}$, were computed for each archetype. Figure 5 shows the collapse assessment results. In detail, Figure 5a shows the collapse fragility curves for BAB (blue line) and BAB+FVD (red line). Estimated parameters $\hat{\theta}$ and $\hat{\beta}$ for the BAB are 0.87 g and 0.27, respectively, whereas for the BAB+FVD are 0.97 g and 0.26, respectively. Comparing the curves, it is evident the better performance of the archetype equipped with FVDs showing a larger $\hat{\theta}$ and lower probabilities at each $S_a(T_1)$ values.

Furthermore, Figure 5b present same collapse fragilities but plotted as function of the inverse of mean annual frequency of exceedance (i.e., $Tr = 1/\lambda_{Sa(T1)}$). This change of variable can be achieved with the information from the hazard curve (green line in Figure 5a). Vertical black lines at reference hazard levels (i.e., Tr equals to 72, 475, 2475 and 4975 years) are also plotted. It is noted that both archetypes have negligible collapse probabilities at SLE and DBE intensities, and small probabilities at MCE and VRE intensities. These modest probabilities will have an important impact on the earthquake-induced repair costs (shown in the subsequent section), since collapse realizations result in losses equal to the building replacement cost.

The collapse fragility can be used to derive additional collapse risk performance metrics such as: i) the collapse margin ratio, CMR; ii) the mean annual frequency of collapse, $\lambda_c$, which represents the average number of collapses per year; and iii) the probability of collapse in the building lifetime (e.g., 50 years), $P_c(50)$, by assuming a Poisson process. CMR estimates were obtained by dividing the respective value of $\hat{\theta}$ by the $S_a(T_1)$ at the MCE level from the hazard curve ($S_a(T_1)_{MCE}$ = 0.34 g, in Figure 5a). CMR values were 2.6 and 2.9 for the BAB and the BAB+FVD, respectively.

Estimated values of $\lambda_c$ and $P_c(50)$ for the BAB were on the order of $2.76\times10^{-5}$ and 0.14%, respectively; while for the BAB+FVD were $1.73\times10^{-5}$ and 0.09%, respectively. The $P_c(50)$ for the BAB is lower than the US-code target of 1% in 50 years [31], and are consistent with the seismic response of modern Chilean RC buildings empirically observed in recent earthquakes. While $P_c(50)$ values are very low, the BAB+FVD shows a reduction on the order of 40% in relation to the BAB. From a point of view of the collapse prevention, these results indicate that the strategy of seismically upgrading Chilean RCWF buildings with FVDs apparently do not represent a meaningful benefit, at least for the high-rise structure at the location and soil type considered in this study. However, further studies will be needed considering other structural systems, heights, seismicity levels, soils, etc. to assess this observation.

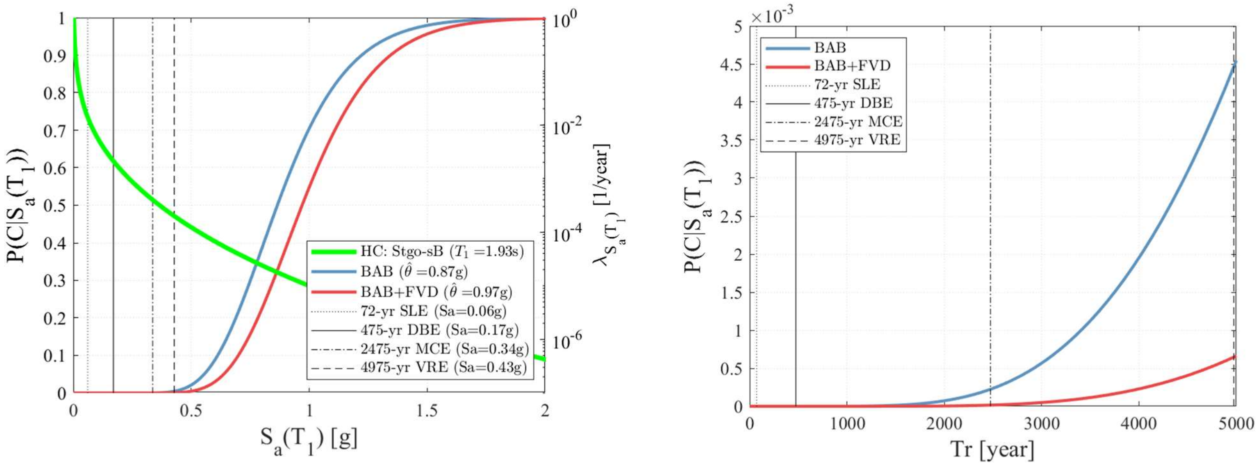


*(a)* *(b)*

*Figure 5. Collapse fragilities in terms of: (a) spectral acceleration at the fundamental period, $S_a(T_1)$, (b) return period, Tr.*

**Economic Loss Assessment**

Four intensity-based assessments were carried out to evaluate the expected performance of the archetypes conditioned on the specified ground shaking intensities: SLE, DBE, MCE, and VRE. This type of evaluation is frequently used in the engineering community to evaluate the seismic performance of new or existing buildings, for example at a design hazard level. The assessment results are reported as the expected consequences in terms of direct economic losses for the BAB and BAB+FVD designs. Furthermore, an additional strategy to achieve increased levels of resilience for both archetypes was considered by improving the seismic performance of nonstructural components, identified as BAB+ENC and BAB+FVD+ENC archetypes. Recent studies have highlighted the benefits of combining enhancement strategies (e.g., for the structural system and for the nonstructural components) in the seismic performance of mid- and high-rise buildings [14], [32].

At each shaking intensity considered in the study, 2000 Monte Carlo simulations were carried out to evaluate the earthquake-induced losses. For each realization, according to the methodology [5], the losses are calculated as follows: i) EDPs are estimated from the results of NLRH analyses; ii) fragility functions are used in conjunction with EDPs to determine the associated damage state for each structural and nonstructural component; iii) consequence functions are then used to translate damage states into repair costs. Then, the direct economic losses for each realization are calculated for every component at every story throughout the building. The loss assessment was carried out using Pelicun software [33]. Fragility and consequence functions of the components were provided by the FEMA P-58 database. Further adjustments will be needed to adapt these functions to the Chilean engineering practice.

A building performance model was created for each archetype. The building replacement cost for the benchmark archetype office building was estimated assuming a cost of US $2,400 per square meter on the basis of the annual statistics of construction costs of the Chile's Ministry of Housing [34]. The cost of the FVDs (including the devices, testing, and additional steel braces) was assumed to be 3% of the BAB construction cost [16]. The cost of the nonstructural-component-enhancement strategy is also taken to be 3% of the BAB construction cost. The latter was estimated on the basis of utilizing nonstructural components with improved seismic behavior might represent an increment of 5% on the total costs of these components in a typical office building [14]. Additionally, recent studies suggest that the cost distribution in Chilean office buildings are approximately 40% and 60% of the total construction cost for structural and nonstructural components, respectively. Regarding the quantities, structural components were based on the structural design and nonstructural component quantities were estimated based on typical quantities found in commercial buildings using the FEMA P-58 Normative Quantity Estimation Tool [5]. The building performance models, with components and quantities, are not show here for brevity.

The EDPs previously defined were used for different building components, based on their capability to predict damage in RC buildings (e.g., drift-sensitive or acceleration-sensitive components). The demand parameters are: PSDR, PSDRt, and PFA. Residual drift was also included in the analysis to account for cases where the building is assumed to be damaged beyond repair and needs to be demolished. This EDP is uncertain and highly sensitive to the nonlinear modeling assumptions and GM characteristics. Hence, it was estimated as a function of PSDR and yield drift following the recommendations [5]. FEMA P-58 also suggests that the building repair fragility be represented by a cumulative lognormal distribution with a median value of

1% residual drift ratio and a dispersion of 0.3. However, after the 2010 earthquake [1] many damaged RC buildings with residual drift ratios larger than 1% were stabilized and repaired in Chile. In this sense, a median value of 1.5% was assumed, but further studies will be needed to refine this assumption. Likewise, the building specific collapse fragilities described ahead were used to determine varying probabilities of collapse at the four intensities. Though the NLRH analyses were conducted in transverse direction, loss estimation requires inputs in both orthogonal directions, thus quantities in the longitudinal direction were also considered. Consequently, EDPs were assumed to be the same in both archetype directions (conservative criterion).

Figure 6 shows the expected (mean) loss ratios under 72-, 475-, 2475-, and 4975-year intensity levels for the benchmark archetype (BAB) as well as the seismically enhanced archetypes (BAB+ENC, BAB+FVD, and BAB+FVD+ENC). From the bar plot, it is seen that the expected repair costs of all archetypes are negligible at the 72-year hazard level (i.e., no more than 0.2% of the building replacement cost). These values are similar to those reported in other studies for RC wall buildings [35], where a predominantly elastic structural response is expected for the service level. Similarly, for the design hazard level, the mean losses are minimal (i.e., no more than 2.3%). These results are consistent with the low EDP responses observed in Figure 3 at both shaking intensities.

On the other hand, at 2475- and 4975-year intensity levels, the expected earthquake-induced repair costs are important. For example, the benchmark archetype (BAB) depicts loss ratios of 13.2% and 30.9% of the building replacement costs for MCE and VRE levels, respectively. However, comparing these values with those reported in other studies for high-rise RC wall buildings under subduction seismicity [36], for the 475-year hazard level, Chilean RC buildings reveal fewer losses than those located in Seattle (i.e., Cascadia subduction zone) and designed to comply with the US code.

Regarding the impact of FVDs, results indicate that seismically improving Chilean RCWF buildings with energy dissipated devices allow expected repair cost reductions on the order of ~50% with respect to those from a conventional design. Certainly, this decrease is more meaningful at extreme intensities (MCE and VRE) than frequent intensities (SLE and DBE). For instance, at MCE intensity, the repair cost drops from 13.2% to 7.7% of the building replacement costs.

Regarding the influence of the enhancement of nonstructural components, results show slight reductions in the repair costs at all intensity levels revealing that there is reduced cost-benefit when applying this strategy, at least for the high-rise structure at the location (Santiago) and soil type (stiff soil) considered in this study. This observation must be considered with caution since further studies will be needed considering RC buildings with different heights, seismicity levels, and soil types. Previous studies with more flexible buildings such as steel moment-frame buildings [14], found more significant decreases with the strategy of improving the seismic performance of the lightweight partitions.

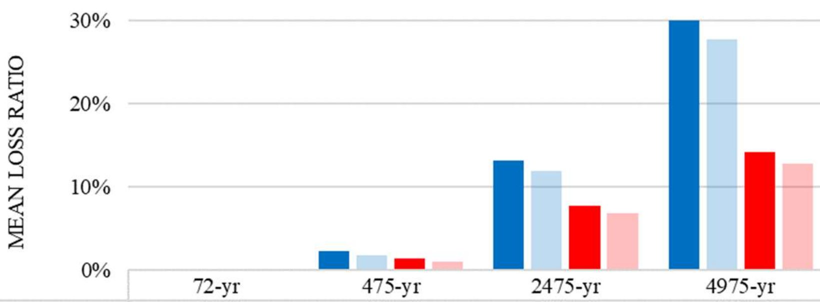


| | 72-yr | 475-yr | 2475-yr | 4975-yr |
|---|---|---|---|---|
| BAB | 0.2% | 2.3% | 13.2% | 30.9% |
| BAB+ENC | 0.2% | 1.8% | 11.9% | 27.7% |
| BAB+FVD | 0.2% | 1.4% | 7.7% | 14.2% |
| BAB+FVD+ENC | 0.1% | 1.1% | 6.8% | 12.8% |

*Figure 6. Mean losses under SLE, DBE, MCE, and VRE intensity levels.*

Additionally, Figure 7 provides the loss breakdown for all archetypes under the four intensities considered. From the bar plot, first, it is identified that the major contributor to the mean loss is repairable damage to structural and nonstructural components for all intensity levels. As seen in the figures for BAB (Figure 7a and 7b), at the 4975-year intensity, irreparable damage is noted as a second contributor caused by residual drifts. By contrast, for BAB+FVD (Figure 7c and 7d), irreparable costs are negligible. This outcome for the archetypes equipped with energy dissipated devices was expected due to the low PRDR responses previously highlighted in Figure 3c. Finally, for all cases there are almost no loss contributions due to collapse since the probabilities of collapse (depicted in Figure 5b) are very low, consistent with empirical observations of the performance of modern Chilean RC buildings. A further evaluation will be needed to study in detail the contributors for the repairable damage (i.e., structural components, and drift- and acceleration-sensitive nonstructural components).

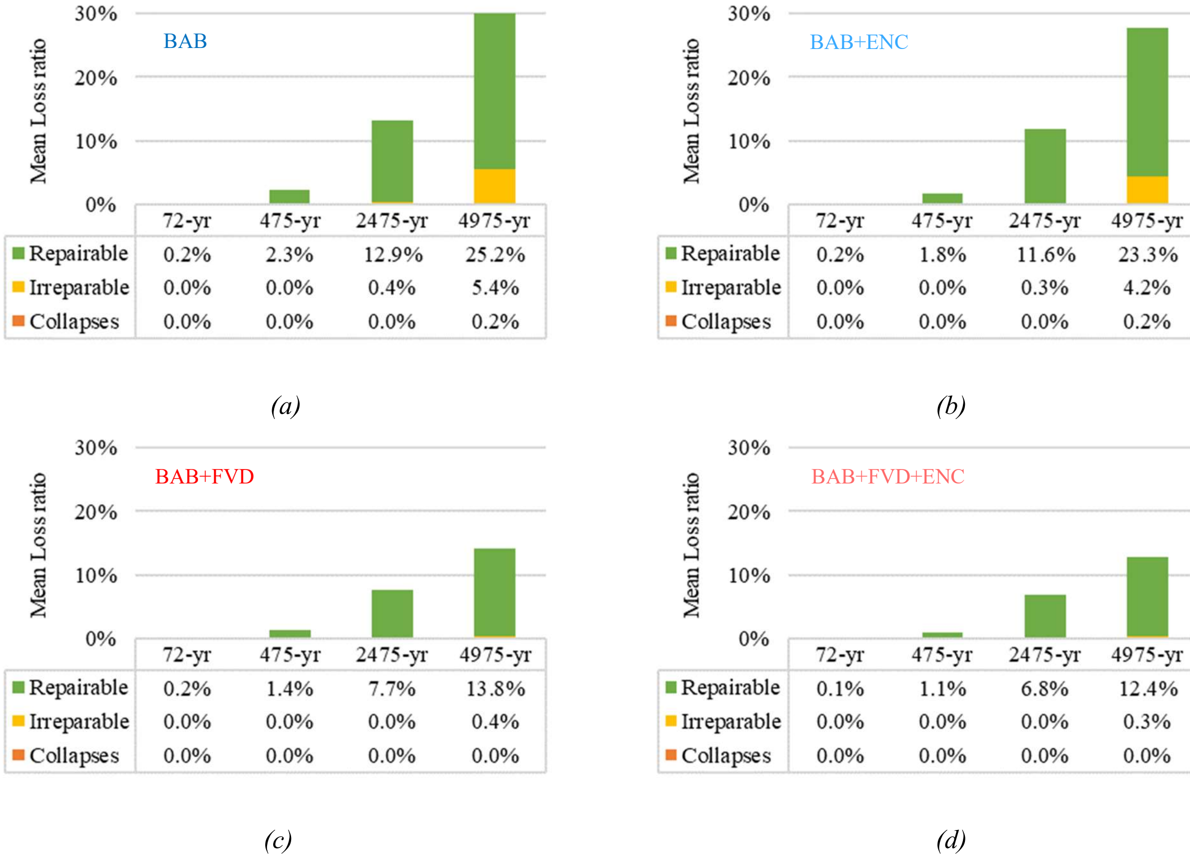


*Figure 7. Mean repair loss breakdown for archetypes: (a) BAB, (b) BAB+ENC, (c) BAB+FVD, (d) BAB+FVD+ENC.*

## CONCLUSIONS

This study evaluates the influence of FVDs on the seismic collapse capacity and direct economic losses of Chilean RC dual wall-frame buildings. As a case study, a high-rise (16-story) office building representative of the Chilean state of design and construction practice was considered. Two cases were analyzed: i) the archetype without dampers, and ii) the same archetype equipped with supplemental FVDs. An alternative strategy to evaluate the seismic performance enhancement of nonstructural components was also explored. The archetypes were located in Santiago (moderate seismicity zone) on stiff soil. Collapse probabilities and expected economic losses were calculated and compared at four hazard intensity levels with return periods of 72, 475, 2475, and 4975 years (i.e., SLE, DBE, MCE, and VRE, respectively) following the FEMA P-58 methodology. The summary of outcomes is as follows:

- Collapse fragility functions were estimated for the buildings with and without FVDs. Median collapse capacity, $\hat{\theta}$, and dispersion, $\hat{\beta}$, for the BAB were 0.87 g and 0.27, respectively, whereas for the BAB+FVD were 0.97 g and 0.26, respectively. Negligible collapse probabilities at SLE and DBE intensities, and very small probabilities at MCE and VRE intensities were noted. From the integration of the collapse fragilities with the hazard curve, mean annual frequency of collapse, $\lambda_c$, and the probability of one collapse in 50 years, $P_c(50)$, were calculated. Values of $\lambda_c$ and $P_c(50)$ for the BAB were $2.76\times10^{-5}$ and 0.14%, respectively; while for the BAB+FVD were $1.73\times10^{-5}$ and 0.09%, respectively. The 50-year probability of collapse of the archetype equipped with FVDs was almost a half of that the benchmark building. In any case, these $P_c(50)$ are lower than the US-code target of 1% in 50 years and are consistent with the seismic response of modern Chilean RC buildings empirically observed in recent earthquakes.
- Expected direct economic losses for all archetypes were negligible at the 72-year hazard level (≤ 0.2% of the building replacement cost) and are minimal (≤ 2.3%) at the 475-year hazard level. On the other hand, at 2475- and 4975-year intensity levels, the economic losses are considerable (13.2% and 30.9%, respectively, for the benchmark archetype). The archetype equipped with FVDs showed repair cost reductions on the order of ~50% with respect to those from a conventional design. Specifically, for the BAB+FVD the repair costs were 1.4%, 7.7%, and 14.2% of the building replacement costs under DBE, MCE and VRE, respectively. Finally, considering the effect of seismically improving nonstructural components, shows slight decreases in the repair costs at all intensity levels. This reveals that there may

be a limited cost-benefit when applying this strategy for this type of RC building since the increment in the initial construction cost could be more than 3%.

The results indicate that seismically enhancing Chilean RC dual wall-frame buildings with seismic protection systems, such as fluid viscous dampers, achieve higher levels of resilience. A beneficial trade-off between higher initial investments and future reduction of the earthquake-induced economic losses is more evident at extreme intensities (MCE and VRE) than frequent intensities (SLE and DBE). Nevertheless, the observations obtained in this study must be judged with caution since further studies will be needed considering buildings with different heights, seismicity levels, and soil types.

## ACKNOWLEDGMENTS

This research was funded by ANID Doctorado Nacional 2018 Folio 21181157, FONDECYT de Iniciación – Grant 11191194, and the Research Center for Integrated Disaster Risk Management (CIGIDEN) ANID FONDAP 1522A0005. Valuable comments on the Chilean seismic design practice were provided by Ian Watt (VMB Structural Engineering) and Mario Lafontaine (Rene Lagos Engineers). The strong motion database was provided by the SIBER-RISK project: Simulation Based Earthquake Risk and Resilience of Interdependent Systems and Networks.

## REFERENCES

[1] EERI. (2010). "The Mw 8.8 Chile Earthquake of 27 February 2010". Earthquake Engineering Research Institute: Oakland, CA, USA.

[2] EERI. (2011). "The M 6.3 Christchurch, New Zealand, Earthquake of February 22, 2011". Earthquake Engineering Research Institute: Oakland, CA, USA.

[3] INE. (2020). Base de Datos de Permisos de Edificación. Instituto Nacional de Estadística: Santiago, Chile. (In Spanish)

[4] CChC. (2012). *Protección Sísmica de Estructuras, Sistemas de Aislación Sísmica y Disipación de Energía*. Corporación de Desarrollo Tecnológico - Cámara Chilena de la Construcción. ISBN: 978-956-7911-19-6. Santiago, Chile. (In Spanish)

[5] FEMA. (2018). *Seismic Performance Assessment of Buildings FEMA P-58*. Federal Emergency Management Agency: Hyattsville, MD, USA.

[6] Lagos, R., Lafontaine, M., Bonelli, P., Boroschek, R., Guendelman, T., Massone, L., Saragoni, R., Rojas, F., Yañez, F. (2021). "The quest for resilience: The Chilean practice of seismic design for reinforced concrete buildings". *Earthq. Spectra*, 37, 26–45.

[7] INN. (2008). *Norma Chilena Oficial NCh 430 Of. 2008 Hormigón armado - Requisitos de diseño y cálculo*. Instituto Nacional de Normalizacion: Santiago, Chile. (In Spanish)

[8] INN. (2009). *Norma Chilena Oficial NCh 433 Of. 1996 Mod. 2009 Diseño Sismico de Edificios*. Instituto Nacional de Normalizacion: Santiago, Chile. (In Spanish)

[9] Saatcioglu, M., Palermo, D., Ghobarah, A, Mitchell, D., Simpson, R., Adebar, P., Tremblay, R., Ventura, C., Hong, H. (2013). "Performance of reinforced concrete buildings during the 27 February 2010 Maule (Chile) earthquake". *Can. J. Civ. Eng.*, 40(8), 693–710.

[10] MINVU. (2011). *DS 60 Requisitos de Diseño y Calculo Para el Hormigón Armado*. Ministerio de Vivienda y Urbanismo: Santiago, Chile. (In Spanish)

[11] MINVU. (2011). *DS 61 Diseño Sísmico de Edificios*. Ministerio de Vivienda y Urbanismo: Santiago, Chile. (In Spanish)

[12] INN. (2013). *Norma Chilena Oficial NCh 2745 Análisis y diseño de edificios con aislación sísmica*. Instituto Nacional de Normalización: Santiago, Chile. (In Spanish)

[13] INN. (2017). *Norma Chilena Oficial NCh 3411 Diseño Sísmico de Edificios con Sistemas Pasivos de disipación de energía - Requisitos y métodos de ensayo*. Instituto Nacional de Normalización: Santiago, Chile. (In Spanish)

[14] Araya-Letelier, G. (2014). "Design of Building Structural Systems and Enhanced Partition Walls to Improve the Life Cycle Costs Associated with Risk of Earthquake Damage". Ph.D. Thesis, Stanford University, Stanford, CA, USA.

[15] Gallegos, M.F., Araya-Letelier, G., Lopez-Garcia, D., Parra, P.F. (2023). "Seismic collapse performance of high-rise RC dual system buildings in subduction zones". *Case Studies in Construction Materials*. 18 (2023), e02042.

[16] Taylor Inc. (2022). *Fluid Viscous Dampers, General Guidelines for Engineers, Including a Brief History*. Taylor Devices Inc.

[17] CSI. (2017). PERFORM 3D 7.0.0 Manual; Computer & Structures: Berkeley, CA, USA.

[18] Lowes, L.N., Lehman, D.E., Baker, C. (2016). "Recommendations for modeling the nonlinear response of slender reinforced concrete walls using PERFORM-3D". *In Proceedings of the SEAOC Convention*. Maui, HI, USA, 12–15 October.

[19] Kolozvari, K., Arteta, C., Fischinger, M., Gavridou, S., Hube, M., Isakovic, T., Lowes, L., Orakcal, K., Vásquez, J., Wallace, J. (2018). "Comparative study of state-of-the-art macroscopic models for planar reinforced concrete walls". *ACI Struct. J.,* 115, 1637–1657.

[20] Ugalde, D., Lopez-Garcia, D. (2020). "Analysis of the seismic capacity of Chilean residential RC shear wall buildings". *J. Build. Eng.*, 31, 101369.

[21] Massone, L.M., Bedecarratz, E., Rojas, F., Lafontaine, M. (2021). "Nonlinear modeling of a damaged reinforced concrete building and design improvement behavior". *J. Build. Eng.*, 41, 102766.

[22] Akcelyan, S., Lignos, D.G., Hikino, T. (2018). "Adaptive numerical method algorithms for nonlinear viscous and bilinear oil damper models subjected to dynamic loading". *Soil Dyn. Earthq. Eng.*, 113 (2018), 488–502.

[23] Kasai, K., Matsuda, K. (2014). "Full-scale dynamic testing of response-controlled buildings and their components: concepts, methods, and findings". *Earthq Eng Eng Vib*. 13(1):167–181.

[24] Zhou, Y., Sebaq, M.S., Xiao, Y. (2022). "Energy dissipation demand and distribution for multi-story buildings with fluid viscous dampers". *Eng. Struct.* 253 (2022), 113813.

[25] Candia, G., Macedo, J., Jaimes, M.A., Magna-Verdugo, C. (2019). "A new state-of-the-art platform for probabilistic and deterministic seismic hazard assessment". *Seismol. Res. Lett*. 90, 226–2275.

[26] Poulos, A., Monsalve, M., Zamora, N., de la Llera, J.C. (2019). "An updated recurrence model for Chilean subduction seismicity and statistical validation of its Poisson nature". *Bull. Seismol. Soc. Am*. 109, 66–74.

[27] Montalva, G.A., Bastías, N., Rodriguez-Marek, A. (2017). "Ground-motion prediction equation for the Chilean subduction zone". *Bull. Seismol. Soc. Am*. 107, 901–911.

[28] Idini, B., Rojas, F., Ruiz, S., Pasten, C. (2017). "Ground motion prediction equations for the Chilean subduction zone". *Bull. Earthq. Eng*. 15, 1853–1880.

[29] Castro, S., Benavente, R., Crempien, J.G.F., Candia, G., de la Llera, J.C. (2022). "A consistently processed strong-motion database for Chilean earthquakes". *Seismol. Res. Lett*. 93, 2700–2718.

[30] Ugalde, D., Parra, P.F., Lopez-Garcia, D. (2019). "Assessment of the seismic capacity of tall wall buildings using nonlinear finite element modeling". *Bull. Earthq. Eng*. 17(12), 6565–6589.

[31] ASCE. (2022). *Minimum Design Loads and Associated Criteria for Buildings and Other Structures ASCE/SEI 7-22*. American Association of Civil Engineers: Reston, VA, USA.

[32] Molina Hutt, C. (2017). "Risk-Based Seismic Performance Assessment of Existing Tall Steel Framed Buildings". Ph.D. Thesis, University College London, London, UK.

[33] Zsarnóczay, A. (2023). "Pelicun, Probabilistic Estimation of Losses, Injuries, and Community resilience Under Natural hazard events". NHERI SimCenter.

[34] MINVU. (2023). *RE 51 Fija Valores Unitarios de Construcción para Aplicar en Cálculo de Derechos de Permisos Municipales*. Ministerio de Vivienda y Urbanismo: Santiago, Chile. (In Spanish)

[35] Arboleda-Monsalve, L.G., Mercado, J.A., Terzic, V., Mackie, K.R. (2020). "Soil–Structure Interaction Effects on Seismic Performance and Earthquake-Induced Losses in Tall Buildings". *J. Geotech. Geoenviron. Eng.* 146(5): 04020028.

[36] Kourehpaz, P., Molina Hutt, C., Marafi, N., Berman, J.W., Eberhard, M.O. (2021). "Estimating economic losses of midrise reinforced concrete shear wall buildings in sedimentary basins by combining empirical and simulated seismic hazard characterizations". *Earthquake Engng Struct Dyn*. 50:26–42.